

Uniform Response Spectrum Method for Seismic Travelling Responses Analysis of Long-span Arch Bridges

M. Lou & Y. Tang

*State Key Laboratory of Disaster Reduction in Civil Engineering,
Tongji University, Shanghai, China*



SUMMARY:

A new symmetrical and anti-symmetrical uniform excitation response spectrum method is proposed for studying the seismic responses of the long-span arch bridge. First, the symmetrical and anti-symmetrical acceleration time-history are obtained depending on the bridge span and the seismic apparent velocity. Then based on the four types of engineering site, both the symmetrical and anti-symmetrical uniform excitation response spectra considering the wave passage effect are established respectively. At last, the seismic responses of a long-span arch bridge under the uniform excitation and the travelling excitation are analyzed. The numerical results show that the method proposed in this paper is a simple and effective technique to evaluate the seismic response of the arch bridges using conventional response spectrum when the wave passage effect must be considered.

Keywords: Long-span bridge; wave passage effect; response spectrum method; uniform excitation; time-history method

1. INSTRUCTIONS

As one of the most important issues of structural dynamic analysis, the effect of ground motion variations on the seismic responses of structures has been studied by many researchers. According to their studies, the variations of ground motion may include the wave passage effect, the partial coherency effect, the effect of wave attenuation and even the local site effect. Especially the wave passage effect should not be ignored when the span of a structure is no less than a quarter of the wavelength. As the effect of wave passage has significant influence on the seismic responses of long-span structures, correctly formulating the set of motions at support points for the long-span structures is important. Response spectrum method (RSM) is world-widely adopted by the seismic design codes of different structures, but the conventional response spectrum method cannot consider the multi-support excitations. So that developing the new response spectrum method considering multi-support excitations (MSRM) is the aim of many scholars. The typical work is the research of Kiureghian and Neuenhofer. Though the suggested MSRM effectively accounts for the contribution of the pseudo-static and dynamic components of responses as well as their covariance, its equation makes the calculation too complicated that it is not yet accepted by practical engineers. Based on the conventional response spectrum method (RSM) and the structural symmetry, a new RSM is developed for seismic response analysis of long-span arch bridge under the multi-support excitations in this paper.

2. S/A-RSM FOR MULTI-SUPPORT SEISMIC RESPONSE ANALYSIS OF ARCH BRIDGE

2.1. Simplified method for seismic responses analysis of arch bridges

We take a simple arch bridge shown in Fig. 2.1 which is excited by ground motions $a_g^1(t)$ and $a_g^2(t)$ to formulate a methodology that converting the seismic response calculation of the whole bridge under

multi-support excitations into that of the symmetrical and anti-symmetrical semi-arch bridges under the uniform excitations $a_s(t)$ and $a_a(t)$ respectively.

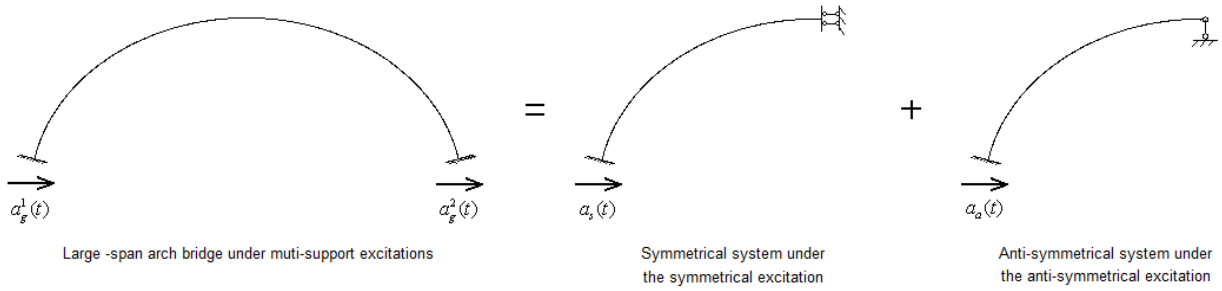


Figure 2.1. Decomposition method drawing

Based on the symmetrical characteristic of the arch bridge, the acceleration excitations $a_s(t)$ and $a_a(t)$ can be obtained by

$$\begin{cases} a_s(t) = \frac{1}{2}[a_g^1(t) - a_g^2(t)] & \text{(for horizontal excitation)} \\ a_a(t) = \frac{1}{2}[a_g^1(t) + a_g^2(t)] \end{cases} \quad (2.1)$$

or

$$\begin{cases} a_s(t) = \frac{1}{2}[a_g^1(t) + a_g^2(t)] & \text{(for vertical excitation)} \\ a_a(t) = \frac{1}{2}[a_g^1(t) - a_g^2(t)] \end{cases} \quad (2.2)$$

where subscripts “s” and “a” denote symmetrical and anti-symmetrical component respectively, $a_g^i(t)$ is the input acceleration at support- i of the bridge. When the uniform excitation is taken into account, $a_g^1(t) = a_g^2(t)$. If the wave passage effect is only considered,

$$a_g^2 = a_g^1 \left(t - \frac{\Delta_{12}}{v_{app}} \right) = a_g \left(t - \frac{\Delta_{12}}{v_{app}} \right) \quad (2.3)$$

where Δ_{12} denotes the horizontal distance between the supports 1 and 2, v_{app} is the surface apparent velocity. $a_g(t)$ is the input seismic acceleration and $a_g^1(t) = a_g(t)$. Then Eqn. 2.1 and Eqn. 2.2 can be rewritten as follows

$$\begin{cases} a_s(t) = a_g^s(t, \Delta_{12}, v_{app}) \\ a_a(t) = a_g^a(t, \Delta_{12}, v_{app}) \end{cases} \quad (2.4)$$

where $a_g^s(t, \Delta_{12}, v_{app})$ and $a_g^a(t, \Delta_{12}, v_{app})$ denote the symmetrical and anti-symmetrical component of input motions.

The equations of motion for the symmetrical and anti-symmetrical semi-arch bridges subject to $a_s(t)$ and $a_a(t)$ respectively can be written in the matrix form

$$\begin{cases} [M_s]\{\ddot{u}_s(t)\} + [C_s]\{\dot{u}_s(t)\} + [K_s]\{u_s(t)\} = -[M_s]\{e_s\}a_s(t) \\ [M_a]\{\ddot{u}_a(t)\} + [C_a]\{\dot{u}_a(t)\} + [K_a]\{u_a(t)\} = -[M_a]\{e_a\}a_a(t) \end{cases} \quad (2.5)$$

where $\{u_s(t)\}$ and $\{u_a(t)\}$ are the displacements of the symmetrical and anti-symmetrical semi-arch bridges, $[M]$, $[C]$ and $[K]$ are the mass, damping and stiffness matrices respectively.

The methodology mentioned above is an accurate calculation method that can be approved by the mechanical theory and numerical results. That is, when a symmetrical structure is under an arbitral two-support seismic excitation, it is feasible to divide the seismic excitation into two parts: the symmetrical excitation (SE) and the anti-symmetrical excitation (AE). Thus, the seismic response of the whole structure can be described as the sum of the responses of the symmetrical semi-structure under the uniform excitation SE and that of the anti-symmetrical one under the uniform excitation AE.

2.2. Symmetrical and anti-symmetrical uniform excitation response spectra

Obviously, two equations of motion in Eqn. 2.5 can be solved by the conventional response spectrum method because the equations describe the structural dynamic responses under the uniform seismic excitation. If the uniform excitation response spectrum corresponding to the symmetrical and anti-symmetrical components $a_s(t)$ and $a_a(t)$ is established respectively, it will be easier to estimate the seismic responses of the long-span arch bridge than the multi-support excitations response spectrum method. As practicing engineers have been so familiar with the application of the uniform excitation response spectrum method, the method suggested in this paper will not have difficulty to apply in engineering. According to the definition of response spectrum, the response spectra corresponding to $a_s(t)$ and $a_a(t)$ respectively are called the symmetrical or anti-symmetrical uniform excitation response spectrum. Obviously, unlike the traditional response spectrum, the spectra named $S_s(\omega, \zeta, \Delta t)$ and $S_a(\omega, \zeta, \Delta t)$ respectively are the functions of parameter $\Delta t = \Delta_{12}/v_{app}$. How to establish the acceleration spectra $S_a^s(\omega, \zeta, \Delta t)$ and $S_a^a(\omega, \zeta, \Delta t)$ will be studied in terms of practical seismic waves from different sites in the next section.

2.3. Qualitative analysis of symmetrical and anti-symmetrical response spectra

The qualitative analysis of response spectrum is a statistical analysis based on the characteristics of earthquakes rather than that of structures. Here, two principles are taken into account: ① the adopted practical seismic waves is obtained according to the Chinese Code for Seismic Design of Building (GB50011-2010), in which four types of soil site are classified including Site I ($V_s > 760 \text{ m}\cdot\text{s}^{-1}$), Site II ($760 \geq V_s > 360 \text{ m}\cdot\text{s}^{-1}$), Site III ($360 \geq V_s \geq 180 \text{ m}\cdot\text{s}^{-1}$) and Site IV ($180 > V_s \text{ m}\cdot\text{s}^{-1}$); ② the number of practical seismic waves from each site is nearly the same. Then, 16 domestic and overseas typical seismic records listed in Tab. 2.1 are used in this study. In order to make the comparison among those spectra more effectively, the amplitudes of recorded seismic waves used in this study are adjusted to 1. Defining ten values of parameter $\Delta t = 0\text{s}$ (equals to the uniform excitation), 0.4s, 0.6s, 0.8s, 1.0s, 1.5s, 2.0s, 2.5s, 3.0s, 4.0s and 5.0s.

Table 2.1. Seismic records from four types of soil site

Site type	I	II	III	IV
Seismic records	F1, F2, N1	F3, F4, F5, N2	F6, F7, F12, N3	F8, F9, F10, F11, N4

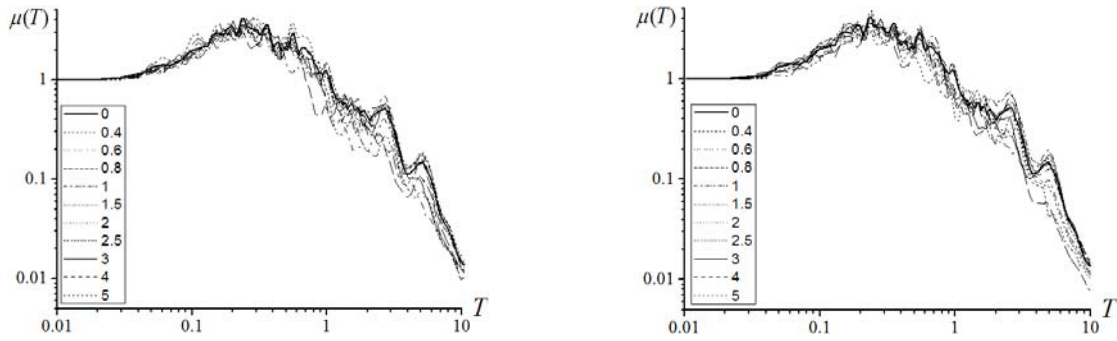
2.3.1. Symmetrical and anti-symmetrical dynamical magnification factor curve

A dynamical magnification factor (DMF) curve $\mu(\omega_i)$ can be defined as the ratio of acceleration amplitude $|\ddot{u}_i(t)|_{\max}$ obtained from a single degree of freedom (SDOF) system divided by the input acceleration amplitude $|a_g(t)|_{\max}$. If SDOF system is linear, it can be expressed by

$$\mu(\omega_i) = \frac{|\ddot{u}_i(t)|_{\max}}{|a_g(t)|_{\max}} = \frac{S_a(\omega_i, \zeta)}{|a_g(t)|_{\max}} \quad (2.6)$$

where, $S_a(\omega_i, \zeta)$ is the acceleration response spectrum of SDOF system; ω_i is the natural frequency of vibration and ζ is the damping ratio.

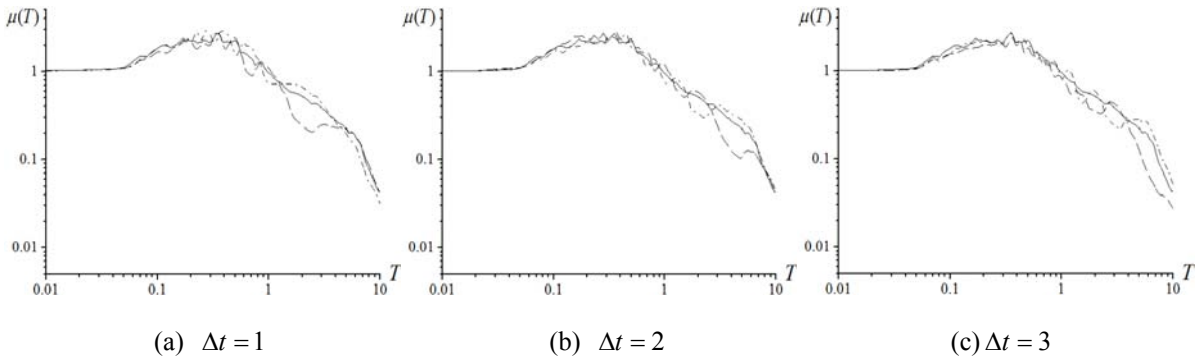
Figs. 2.2 only give the symmetrical and anti-symmetrical DMF curves of F1 from Site I due to the paper space limitation. Here, $\zeta=0.05$. The x -axis denotes natural vibration period T from 0.01s to 10s; the y -axis denotes the dynamical magnification factor curve $\mu(T)$. In Fig. 2.2 (a) and Fig. 2.2 (b), the symmetrical and anti-symmetrical DMF curves with different Δt including $\Delta t=0$ which represents the uniform excitation DMF curve are given respectively.



(a) Anti-symmetrical DMF curves of F1 with different Δt (b) Symmetrical DMF curves of F1 with different Δt

Figure 2.2. The symmetrical and anti-symmetrical DMF curves of F1 from Site I

In Figs. 2.2, it is clear to see that the symmetrical and anti-symmetrical DMF curves $\mu_{\Delta t \neq 0}(T)$ with different parameters Δt are almost of a similar shape as the uniform excitation DMF curve $\mu_{\Delta t=0}(T)$ and the values of $\mu_{\Delta t \neq 0}(T)$ fluctuate around that of $\mu_{\Delta t=0}(T)$. The symmetrical or anti-symmetrical DMF average curves $\bar{\mu}_{\Delta t \neq 0, i}^s(T)$ and $\bar{\mu}_{\Delta t \neq 0, i}^a(T)$ with different Δt are computed for four site respectively. As well as the uniform excitation DMF average curve $\bar{\mu}_{\Delta t=0, i}(T)$ is calculated for comparison. When $\Delta t=1s, 2s, 3s$, the computed results $\bar{\mu}_{\Delta t \neq 0, i}^s(T)$ and $\bar{\mu}_{\Delta t \neq 0, i}^a(T)$ of Site I are shown in Figs. 2.3 represented by dashed lines and dash-dot lines respectively. Meanwhile, black solid line represents the $\bar{\mu}_{\Delta t=0, i}(T)$. It is obvious from Figs. 2.3 that the difference between $\bar{\mu}_{\Delta t \neq 0, i}(T)$ and $\bar{\mu}_{\Delta t=0, i}(T)$ is small and can be considered that $\bar{\mu}_{\Delta t \neq 0, i}(T)$ and $\bar{\mu}_{\Delta t=0, i}(T)$ are same for engineering application. The conclusion for other three sites is same, so that the results are not listed in the paper.



(a) $\Delta t = 1$

(b) $\Delta t = 2$

(c) $\Delta t = 3$

Figure 2.3. Average dynamical magnification factor curves of Site I

2.3.2. Symmetrical and anti-symmetrical amplitude attenuating curves

According to Eqn. 2.6, the input acceleration amplitudes of the symmetrical and anti-symmetrical $a_s(t)$ and $a_a(t)$ are the key to make the current RSM feasible for the dynamic analysis of the arch

bridges under two-support excitations. The amplitudes $A_{i,j}^s(\Delta t)$ and $A_{i,j}^a(\Delta t)$ of symmetrical $a_s(t)$ and anti-symmetrical $a_a(t)$ for four sites can be obtained. Where, i denotes Site i (I-IV); j denotes the name of waves. Due to limited paper space, only one wave from four sites is shown in Tab. 2.2.

Table 2.2. Symmetrical and anti-symmetrical amplitude (cm/s²)

Δt	Site I		Site II		Site III		Site IV	
	$A_{I,F1}^s(\Delta t)$	$A_{I,F1}^a(\Delta t)$	$A_{II,F3}^s(\Delta t)$	$A_{II,F3}^a(\Delta t)$	$A_{III,F6}^s(\Delta t)$	$A_{III,F6}^a(\Delta t)$	$A_{IV,F10}^s(\Delta t)$	$A_{IV,F10}^a(\Delta t)$
0.0	--	147.06	--	265.40	--	1137.8	--	268.44
0.4	125.192	115.61	209.55	154.30	695.49	460.56	211.76	118.06
0.6	106.015	102.68	206.80	136.35	728.39	650.23	202.03	128.59
0.8	118.321	110.99	144.45	231.00	575.54	637.55	127.90	184.65
1.0	98.708	107.06	152.25	199.95	599.90	799.55	150.79	193.03
1.5	119.31	111.73	170.75	169.15	662.31	606.14	164.81	132.19
2.0	122.63	118.12	189.35	132.70	592.19	608.57	134.59	180.20
2.5	103.60	105.07	138.70	160.90	584.15	595.25	187.37	122.34
3.0	105.95	110.49	163.65	202.85	622.34	591.98	159.39	130.74
4.0	98.916	111.42	142.45	132.70	579.29	568.92	159.96	147.88
5.0	101.23	114.07	132.70	181.65	577.62	568.92	111.68	168.78

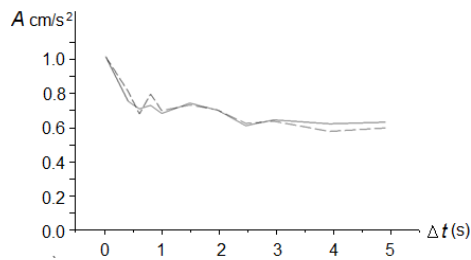
In order to make the data from the tables above be compared with each other, they should be transformed by Eqn. 2.7 and Eqn. 2.8. First, dividing the symmetrical and anti-symmetrical acceleration amplitudes ($\Delta t \neq 0$) by the uniform acceleration amplitude ($\Delta t = 0$), and then calculating the average of $\tilde{A}_{i,j}^{s/a}(\Delta t)$ from each site and still taking Δt as variables.

$$\tilde{A}_{i,j}^{s/a}(\Delta t) = \frac{A_{i,j}^{s/a}(\Delta t)}{A_{i,j}^{s/a}(\Delta t = 0)} \quad (2.7)$$

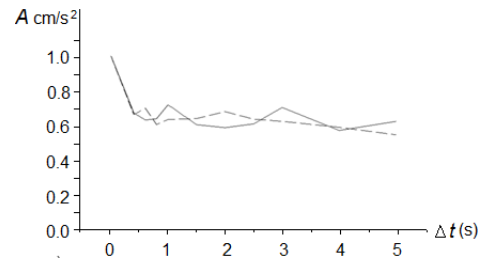
$$\bar{A}_i^{s/a}(\Delta t) = \frac{\sum_{j=1}^n \tilde{A}_{i,j}^{s/a}(\Delta t)}{n} \quad (2.8)$$

where, $\tilde{A}_{i,j}^{s/a}(\Delta t)$ is a function of Δt and begins with 1; n is the number of waves from the same site.

The following figures show the average amplitudes of symmetrical and anti-symmetrical input components of four sites. Dashed line stands for symmetrical component and solid line stands for anti-symmetrical component.



(a) Site I



(b) Site II

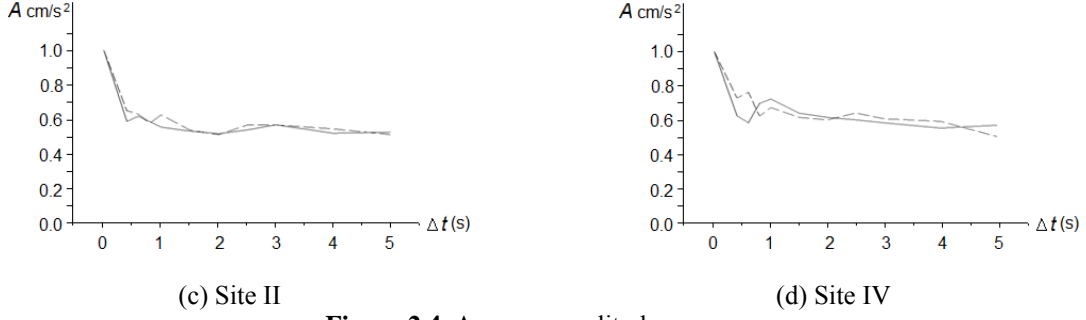


Figure 2.4. Average amplitude curves

Figs. 2.4 illustrate that: ① in general, the symmetrical and anti-symmetrical average amplitudes of four sites decrease when Δt increases; ② when $\Delta t=0\sim 1s$, the curves decrease sharply while the pitch becomes slowly when $\Delta t>1s$. In order to make amplitude attenuation curves easier for application, the fitting attenuating equations $y_{i,s}(\Delta t)$ and $y_{i,a}(\Delta t)$ of the symmetrical and anti-symmetrical average amplitudes for four sites are written as follows.

$$y_{I,s}(\Delta t) = \begin{cases} e^{0.5\Delta t^2 - 0.82\Delta t} & 0 \leq \Delta t < 1 \\ e^{0.009\Delta t^2 - 0.09\Delta t - 0.27} & \Delta t \geq 1 \end{cases} \quad (2.9a)$$

$$y_{I,a}(\Delta t) = \begin{cases} e^{0.6\Delta t^2 - 0.9\Delta t} & 0 \leq \Delta t < 1 \\ e^{0.006\Delta t^2 - 0.06\Delta t - 0.29} & \Delta t \geq 1 \end{cases} \quad (2.9b)$$

$$y_{II,s}(\Delta t) = \begin{cases} e^{0.6\Delta t^2 - 0.95\Delta t} & 0 \leq \Delta t < 1 \\ e^{-0.003\Delta t^2 - 0.04\Delta t - 0.33} & \Delta t \geq 1 \end{cases} \quad (2.10a)$$

$$y_{II,a}(\Delta t) = \begin{cases} e^{0.6\Delta t^2 - 0.95\Delta t} & 0 \leq \Delta t < 1 \\ e^{0.005\Delta t^2 - 0.05\Delta t - 0.34} & \Delta t \geq 1 \end{cases} \quad (2.10b)$$

$$y_{III,s}(\Delta t) = \begin{cases} e^{0.6\Delta t^2 - 1.1\Delta t} & 0 \leq \Delta t < 1 \\ 0.57 & \Delta t \geq 1 \end{cases} \quad (2.11a)$$

$$y_{III,a}(\Delta t) = \begin{cases} e^{0.6\Delta t^2 - 1.1\Delta t} & 0 \leq \Delta t < 1 \\ e^{0.005\Delta t^2 - 0.05\Delta t - 0.45} & \Delta t \geq 1 \end{cases} \quad (2.11b)$$

$$y_{IV,s}(\Delta t) = \begin{cases} e^{0.5\Delta t^2 - 0.9\Delta t} & 0 \leq \Delta t < 1 \\ e^{-0.01\Delta t^2 - 0.001\Delta t - 0.4} & \Delta t \geq 1 \end{cases} \quad (2.12a)$$

$$y_{IV,a}(\Delta t) = \begin{cases} e^{0.55\Delta t^2 - 0.95\Delta t} & 0 \leq \Delta t < 1 \\ e^{0.01\Delta t^2 - 0.09\Delta t - 0.33} & \Delta t \geq 1 \end{cases} \quad (2.12b)$$

2.3.3. Symmetrical and anti-symmetrical response spectrum

The aim of introducing amplitude attenuating curves is to correct the current RSM which is only fitted for the uniform excitation response spectrum analysis and cannot consider the wave passage effect. The amplitude attenuating curve can be used as a kind of correction factor to provide a simplified RSM considering the wave passage effect for traveling seismic response analysis of the structures with

only two supports. The response spectra of symmetrical and anti-symmetrical input components of the traveling seismic inputs can be obtained by multiplying the uniform response spectrum $S_a(\omega, \zeta)$ by amplitude attenuating factors $y_{i,s}(\Delta t)$ and $y_{i,a}(\Delta t)$ respectively. That is,

$$S_a^s(\omega, \zeta, \Delta t) = y_{i,s}(\Delta t) \times S_a(\omega, \zeta) \quad (2.13a)$$

$$S_a^a(\omega, \zeta, \Delta t) = y_{i,a}(\Delta t) \times S_a(\omega, \zeta) \quad (2.13b)$$

2.3.4. S/A-RSM for traveling seismic response analysis of arch bridges

Based on Eqns. 2.13, the seismic responses v_{\max}^s and v_{\max}^a of the arch bridge under the symmetrical and anti-symmetrical excitations can be obtained by RSM. The total seismic response v_{\max} of the arch bridge under the traveling seismic inputs can be calculated by the square root of the sum of the squares (SRSS):

$$v_{\max} \doteq \sqrt{(v_{\max}^s)^2 + (v_{\max}^a)^2} \quad (2.14)$$

The simplified analysis procedure suggested above is called the symmetrical and anti-symmetrical uniform excitation response spectrum method (S/A-RSM).

3. A CASE STUDY FOR S/A-RSM

3.1. Project profile and finite element model

The bridge shown in Fig. 3.1 is a prestressed concrete (PC) T-girder structure. The main span of the arch with 14 bridge openings is $14 \times 30.668\text{m} = 429.4\text{m}$ long. The beam element model for the bridge is shown in Fig. 3.2.

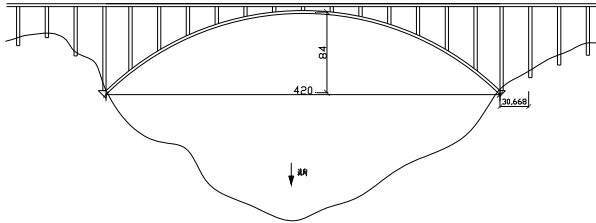


Figure 3.1. Prestressed concrete bridge

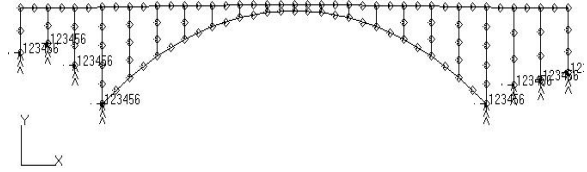


Figure 3.2. Structural finite element model

3.2. Seismic responses of the bridge

Three seismic records of Site IV including Western Washington wave (the duration time is 89.16s), Westmoreland wave (the duration time is 88.44s) and Coalinga wave (the duration time is 65.02s) are adopted in the study. In the calculation, $v_{app} = \infty$ (uniform input), 2000m/s, 1000m/s and 500m/s (that is $\Delta t = 0\text{s}, 0.21\text{s}, 0.42\text{s}, 0.84\text{s}$) are considered. The peak values of acceleration ($a \text{ m/s}^2$) and displacement ($d \text{ m}$) of the bridge subject to the three waves obtained by S/A-RSM are shown in Tabs. 3.1-3.3. In the Tables, HD and VD denote horizontal direction and vertical direction respectively. In the computation, the response spectrum is calculated directly from the three seismic waves respectively. The relative errors of the peak values compared with results computed by step-by-step method (THM) are also listed in the Tables. In the following work, the standard spectrum in China code is used instead of the special response spectrum of the three seismic waves. The peak values of the seismic response of the bridge obtained by S/A-RSM are listed in Tab. 3.4 when input seismic acceleration peak value is equal to 0.2g. The peak values of the seismic responses computed by THM

are the average values from the results when adjusting amplitudes of the three seismic waves to 0.2g.

Table 3.1. Peak values of the arch obtained by S/A-RSM subject to Western Washington wave

Response	Location	Peak values of seismic response				Relative error compared to THM (%)			
		Uniform	2000m/s	1000m/s	500m/s	Uniform	e ₂₀₀₀	e ₁₀₀₀	e ₅₀₀
<i>a</i> (m/s ²)	1/4-span, HD	1.501	3.107	2.423	2.351	10.9	73.5	42.7	31.7
	1/4-span, VD	1.212	1.195	1.169	1.120	69.3	-13.7	-16.5	-17
	1/2-span, HD	2.124	1.312	1.193	1.432	42.6	6.90	13.9	35.9
	1/2-span, VD	0.000	1.280	1.096	1.246	--	-6.77	-24.4	-16.8
<i>d</i> (m)	1/4-span, HD	0.032	0.030	0.027	0.019	146.7	36.4	0	-36.7
	1/4-span, VD	0.052	0.050	0.045	0.030	18.8	56.3	15.4	-21.1
	1/2-span, HD	0.026	0.025	0.022	0.015	13.0	19.5	15.8	25.0
	1/2-span, VD	0.000	0.014	0.019	0.022	--	-75.0	-80.0	-84.9

Table 3.2. Peak values of the arch obtained by S/A-RSM subject to Westmoreland wave

Response	Location	Peak values of seismic response				Relative error compared to THM (%)			
		Uniform	2000m/s	1000m/s	500m/s	Uniform	e ₂₀₀₀	e ₁₀₀₀	e ₅₀₀
<i>a</i> (m/s ²)	1/4-span, HD	2.551	5.348	4.147	4.598	-10.3	75.3	7.00	18.8
	1/4-span, VD	2.147	2.384	2.241	2.141	32.4	-12.3	-41.9	-46.7
	1/2-span, HD	3.489	2.423	2.367	2.407	30.6	51.1	15.1	18.7
	1/2-span, VD	0.000	1.771	1.901	1.840	--	-42.2	-58.7	-64.2
<i>d</i> (m)	1/4-span, HD	0.035	0.032	0.027	0.026	169.2	-36.0	-62.5	-65.8
	1/4-span, VD	0.053	0.051	0.044	0.035	194	-25.0	-55.5	-65.0
	1/2-span, HD	0.027	0.024	0.019	0.015	-6.9	-4.00	0	-6.25
	1/2-span, VD	0.000	0.031	0.053	0.061	--	-71.8	-72.8	-77.6

Table 3.3. Peak values of the arch obtained by S/A-RSM subject to Coalinga wave

Response	Location	Peak values of seismic response				Relative error compared to THM (%)			
		Uniform	2000m/s	1000m/s	500m/s	Uniform	e ₂₀₀₀	e ₁₀₀₀	e ₅₀₀
<i>a</i> (m/s ²)	1/4-span, HD	2.007	2.248	2.017	1.588	-12.4	16.4	42.5	-24.8
	1/4-span, VD	1.494	1.332	1.517	1.184	25.0	-43.1	-42.7	-35.9
	1/2-span, HD	2.724	1.168	1.553	1.400	23.7	25.3	53.7	-0.92
	1/2-span, VD	0.000	1.473	1.406	1.473	--	-23.1	-40.1	-41.7
<i>d</i> (m)	1/4-span, HD	0.027	0.025	0.021	0.020	145	-19.4	-50.0	-52.3
	1/4-span, VD	0.041	0.040	0.037	0.028	185	-6.90	-37.3	-52.5
	1/2-span, HD	0.021	0.019	0.016	0.013	23.5	26.7	45.5	8.30
	1/2-span, VD	0.000	0.022	0.033	0.035	--	-63.3	-71.5	-76.5

Table 3.4. Average response values of the bridge obtained by S/A-RSM

Response	Location	Spectrum	Peak values of seismic response				Error compared to THM (%)			
			Uniform	2000m/s	1000m/s	500m/s	Uniform	e ₂₀₀₀	e ₁₀₀₀	e ₅₀₀
<i>a</i> (m/s ²)	1/4-span, HD	AS	0.977	0.603	0.580	0.640	-3.9	28.7	47.6	17.6
		SS	0.539	0.457	0.406	0.373	-48.1	-22.4	-10.4	-42.5
	1/4-span, VD	AS	0.698	0.469	0.471	0.468	27.8	-33.7	-40.2	-25.8
		SS	0.503	0.426	0.379	0.348	-7.90	-54.3	-66.8	-61.3
	1/2-span, HD	AS	0.977	0.603	0.580	0.640	-3.90	28.7	47.6	17.6
		SS	0.539	0.457	0.406	0.373	-48.1	-22.4	-10.4	-42.5
	1/2-span, VD	AS	0.698	0.469	0.471	0.468	27.8	-33.7	-40.2	-25.8
		SS	0.503	0.426	0.379	0.348	-7.90	-54.3	-66.8	-61.3
<i>d</i> (m)	1/4-span, HD	AS	0.016	0.015	0.013	0.010	100.0	0	-31.6	-44.4
		SS	0.029	0.025	0.022	0.021	262.5	40.0	-1.90	-22.2
	1/4-span, VD	AS	0.025	0.024	0.022	0.014	150.0	20.0	-24.1	-44.0
		SS	0.048	0.041	0.037	0.034	380.0	75.0	-6.80	-12.0
	1/2-span, HD	AS	0.013	0.012	0.011	0.007	18.2	9.10	22.2	16.7
		SS	0.024	0.020	0.018	0.017	118.2	54.5	44.4	83.3
	1/2-span, VD	AS	0.000	0.008	0.013	0.014	--	-75.8	-78.3	-85.1
		SS		0.011	0.010	0.095		-69.7	-86.7	-93.6

The results indicate that there are some differences between the calculated errors obtained by S/A-RSM and the current RSM, but they are in the same error level, especially maximum errors appear in RSM. So the S/A-RSM suggested in the paper is still acceptable in engineering application.

4. CONCLUSION

Based on the symmetrical characteristics of the arch bridge, the symmetrical and anti-symmetrical uniform excitation response spectrum method (S/A-RSM) is suggested in the paper for considering the wave passage effect on the seismic responses of long-span arch bridge. The results show that:

(1)The symmetrical and anti-symmetrical response spectra are the functions of the seismic apparent velocity and the bridge span. The longer the span is, the effect of travelling waves on the long-span structure become more significant and cannot be ignored.

(2)The symmetrical and anti-symmetrical dynamical magnification factor curves based on the four types of engineering site have a nice agreement with the uniform excitation DMF curve, which means that the RSM introduced in the design code can still be adopted for dynamic response analysis of structures under multi-support excitations.

(3)The numerical results show that the S/A-RSM is an effective simplified RSM that it can be easily used in engineering, and it is also useful for analyzing the traveling seismic response analysis of other long-span structures with two supports.

ACKNOWLEDGEMENT

This research was sponsored by State Key Laboratory Basic Theory Foundation of the Ministry of Science and Technology of China through a grant SLDRCE08-A-07 and National Natural Science Foundation of China through a grant 90915011. These supports are gratefully acknowledged.

REFERENCES

- He, Q. (2009). Review of structural seismic analysis of travelling wave effects. *Journal of Earthquake Engineering and Structural Vibration*. **29:1**, 50-56.
- Zhong, W. (2000). Development and tendency of the antiseismic design of the long-span structure. *Science & Technology Review*. **21:3**, 7-10.
- Kiureghian, A.D. and Neuenhofer, A. (1996). A coherency method for spatially varying ground motions. *Earthquake Engineering and Structural Dynamics*. **25:1**, 99-111.
- Kiureghian, A.D. and Neuenhofer, A. (1992). Response spectrum method for multi-support seismic excitations. *Earthquake Engineering and Structural Dynamics*. **21:8**, 713-40.
- Heredia-Zavoni, E. and Vanmarcke, E.H. (1994). Seismic random-vibration analysis of multi-support structural systems. *Journal of Engineering Mechanics*. ASCE. **120:5**, 1107-28.
- Lou, M. and Gao, S. (2009). The simplified method for the vertical seismic response analysis of the arch bridge under the multiple-support excitation. *Journal of Disaster Prevention and Mitigation Engineering*. **29:6**, 638-643.
- Biot, M.A. (1941). A mechanical analysis for prediction of earthquake stress. *Bull. Seism. Soc. Am.* **31:1**, 151-171.
- China Academy of Building Research. (2010). Code for seismic design of buildings GB50011-2010. Beijing: China Architecture & Building Press.
- Xie, L. and Zhai, C. (2003). Study on the most unfavorable ground motions in seismic design. *ACTA Seismologica Sinica*. **25:3**, 250-261.
- Clough, R. W. and Penzien, J. (1993). Dynamics of Structures. New York: McGraw-Hill Inc.